RESEARCH PAPER

In-Vivo Antimicrobial Efficacy of Silver Nanoparticles-Loaded Hydrogel Dressings in Burn Wound Infections in Mice

Tripuramallu Rajithasree[1], Pooja Karadi[2], Raosaheb Y. Ghegade[3], Jothika P[4], Sandip Ashok Murtale[5], Janane Murugesan[6], Ritismita Devi[7], Jeyaprakash MR[8*]

[1]Assistant Professor, Chilkur Balaji College of Pharmacy, RangaReddy, Telangana, 500075, India

[2]Assistant Professor, HKES Matoshree Taradevi Rampure, Institute of Pharmaceutical Sciences, Kalaburgi, Karnataka, 585102, India

[3]Associate Professor, Gokhale Education Society's, Sir Dr. M. S. Gosavi College of Pharmaceutical Education & Research, Nashik, Maharashtra, 422005, India

[4]Assistant Professor, Faculty of pharmacy SBMCH Bharath University, Chennai, Tamil Nadu, 600044, India

[5]Professor, Sanjay College of Pharmacy, RGUHS Bangalore, Belgaum, Karnataka, India

[6]Research Scholar, Department of Pharmacy Practice, JSS College of Pharmacy, JSS Academy of Higher Education and Research, Ooty, Tamil Nadu, 643001, India

[7]Assistant Professor, Assam Down Town University, Kamrup Metro, Assam, 781026, India

[8]Professor, MB School of Pharmaceutical Sciences, Mohan Babu University, Sree Sainath Nagar, Tirupati, Chittoor, Andhra Pradesh, 517102, India

***Corresponding author:** Jeyaprakash MR, Professor, MB School of Pharmaceutical Sciences, Mohan Babu University, Sree Sainath Nagar, Tirupati, Chittoor, Andhra Pradesh, 517102, India

Abstract:

Prolonged healing and the emergence of antibiotic resistance render burn wound infections a significant challenge in clinical practice. This study aimed to evaluate the efficacy of hydrogel dressings infused with silver nanoparticles (AgNPs) as an antibacterial agent in a murine model of burn wound infection. A biocompatible hydrogel matrix was employed to synthesize silver nanoparticles, which then underwent physicochemical characterization and antibacterial evaluation. Staphylococcus aureus and Pseudomonas aeruginosa were administered to mice via full-thickness burn wounds. Four groups of animals were selected for the experiment: control, plain hydrogel, standard therapy (silver sulfadiazine), and hydrogel infused with AgNPs. The therapy was applied topically once daily for fourteen days. A 3.2 log reduction in bacterial load was seen in the AgNP-loaded hydrogel group relative to the control group ($p < 0.001$), signifying potent antibacterial efficacy. After 14 days, the treated group exhibited significantly greater wound contraction (92.4%) compared to the plain hydrogel (71.6%), conventional treatment (85.3%), and control (54.2%) groups. The epithelialization period in the control group was 16.5 ± 1.2 days, whereas in the AgNP group, it decreased to 11.2 ± 0.8 days. Histopathological studies indicated that the AgNP-treated group exhibited superior tissue regeneration, reduced inflammatory infiltration, and increased collagen deposition. This study offers promising prospects for the management of infected burn wounds, demonstrating that hydrogel dressings infused with AgNPs exhibit potent antibacterial efficacy and significantly accelerate the healing process.

Keywords: Silver nanoparticles, hydrogel dressing, burn wound, antimicrobial activity, wound healing, mice model

How to cite this article: Rajithasree T, Karadi P, Ghegade RY, Jothika P, Murtale SA, Murugesan J, Devi R, MR J. In-Vivo Antimicrobial Efficacy of Silver Nanoparticles-Loaded Hydrogel Dressings in Burn Wound Infections in Mice. Int J Drug Deliv Technol. 2026;16(16s): 625. DOI: 10.25258/ijddt.16.16s.69

Introduction:

Burn injuries result in significant pain and mortality globally, particularly in underprivileged countries. Burn victims have heightened susceptibility to infection, delayed wound healing, and potential systemic complications due to the disruption of the

skin's protective barrier following the injury. Staphylococcus aureus and Pseudomonas aeruginosa, two of the most common pathogens in burn wound infections, are exhibiting heightened resistance to the antimicrobials employed for their treatment [1, 2].

Alongside microbial control, facilitating tissue regeneration is crucial for the efficient therapy of burn wound infections. Traditional belief posited that silver sulfadiazine and other topical antimicrobials represented the gold standard; nevertheless, research has associated their prolonged use with cytotoxicity, delayed epithelialization, and the emergence of resistant bacteria. Due to these limitations, novel therapeutic strategies are necessary to enhance wound healing while simultaneously including robust antibacterial properties [3].

Nanotechnology has recently garnered attention as a prospective approach for biomedical applications, particularly in wound care. The extensive antibacterial efficacy of silver nanoparticles (AgNPs), particularly against antibiotic-resistant bacteria, has garnered significant interest. AgNPs exert antimicrobial effects through the disruption of bacterial cell membranes, generation of reactive oxygen species, interference with cellular metabolism, and inhibition of DNA replication [4].

Hydrogel wound dressings, composed of three-dimensional hydrophilic polymer networks, are advantageous due to their high-water retention capacity. Besides enabling gas exchange and maintaining a humid environment, they also promote cell migration and proliferation. The integration of the hydrogels' structural and regenerative qualities with the antibacterial efficacy of nanoparticles establishes a synergistic strategy when silver nanoparticles are included into hydrogel systems [5, 6].

Despite several in vitro studies demonstrating their antibacterial properties, comprehensive in vivo testing remains essential to validate the efficacy of AgNPs in treating infected burn wounds. The objective of this study was to evaluate the efficacy of hydrogel dressings infused with silver nanoparticles as an antibacterial agent in a murine model of burn wound infection. The objectives of the study are to assess the impact of treatment on bacterial load, wound contraction, time to epithelialization, and histological changes [7].

Material and Methods:

Materials:

Sodium borohydride ($NaBH_4$), silver nitrate ($AgNO_3$), and additional analytical-grade chemicals were acquired from reputable suppliers. Certified vendors provided the polymers (including carbopol 940, chitosan, and polyvinyl alcohol) used to manufacture the hydrogel. Our microbiological medium, comprising nutrient agar and Mueller-Hinton broth, were procured from HiMedia Laboratories in India. The reference medication employed was 1% w/w silver sulfadiazine cream, a conventional antibiotic.

Synthesis of Silver Nanoparticles (AgNPs):

The chemical reduction approach was used to manufacture silver nanoparticles. I made a 1 mM solution of silver nitrate and reduced it with newly generated sodium borohydride while stirring continuously at 4°C. The presence of AgNPs was confirmed when the reaction mixture underwent a color change from colorless to pale yellow-brown. In order to lyophilize the nanoparticles, they were first centrifuged at 15,000 rpm for 20 minutes, then rinsed with distilled water [8].

Characterization of AgNPs:

Spectroscopic and microscopic methods were used to thoroughly examine the produced silver nanoparticles, verifying their shape, size distribution, surface charge, and formation.

UV–Visible Spectroscopy:

Surface plasmon resonance (SPR) served as the foundational principle for the UV-Visible spectroscopy validation of silver nanoparticle synthesis. The UV-Vis spectrophotometer recorded the absorbance spectra of the synthesized AgNPs within the 300-700 nm wavelength range. A prominent absorption peak at around λmax = 420 nm is characteristic of spherical silver nanoparticles. Upon exposure to incoming light, the conduction band electrons at the nanoparticle's surface fluctuate collectively, producing this peak. The reaction mixture's transition to a pale yellow to

brown tint indicated the creation of nanoparticles. A crisp and symmetrical absorption peak indicated a rather uniform size distribution, but a widened peak suggested the presence of polydispersity or aggregation. The synthesized nanoparticles were confirmed to be pure and stable due to the absence of any additional peaks [9, 10].

Dynamic Light Scattering (DLS):

Dynamic light scattering (DLS) was employed to determine the hydrodynamic diameter and polydispersity index (PDI) of the AgNPs. The nanoparticle solution was properly diluted with deionized water, and the analysis was conducted at 25°C. The synthesized AgNPs exhibited nanoscale dimensions suitable for biological applications, with an average particle size between 20 and 80 nm. The nanoparticle consistency was exceptional, and the size distribution was narrow, as shown by a PDI value of less than 0.3. The hydrodynamic size, determined by DLS, encompasses the core nanoparticle, adsorbed molecules, and solvent layers. Consequently, DLS typically produces slightly larger measurements than electron microscopy. The synthesis method effectively generated nanoparticles with minimal aggregation and a predominantly monodisperse distribution, as indicated by the low PDI value [11].

Zeta Potential Analysis:

The zeta potential of the synthesized AgNPs was assessed to evaluate their surface charge and colloidal stability. An electrophoretic mobility-based zeta potential analyzer was utilized for the analysis. The AgNPs exhibited a significant negative surface charge, indicated by a zeta potential value of approximately -25 to -35 mV. The synthesis of nanoparticles entails the adsorption of stabilizing agents or ions onto their surfaces, which imparts a negative charge to them. Effective colloidal stability, maintained by electrostatic repulsion among particles, is often signified by a zeta potential magnitude above ±20 mV. Consequently, the results confirmed the physical stability and uniform dispersion of the synthesized AgNPs in the solution [12].

Transmission Electron Microscopy (TEM):

Transmission electron microscopy (TEM) was employed to examine the morphology and exact dimensions of the AgNPs. A carbon-coated copper grid was subjected to a drop of diluted nanoparticle suspension, allowed to dry at room temperature, and subsequently analyzed with a transmission electron microscope. TEM scans revealed that most of the synthesized AgNPs were spherical, exhibited smooth surfaces, and were uniformly distributed inside the material, exhibiting minimal aggregation. Particle sizes were ascertained to be 15-50 nm, slightly smaller than the DLS results due to the absence of the hydration layer in the TEM analysis. Additional validation of the successful synthesis of stable and monodisperse silver nanoparticles was evidenced by the narrow size distribution and consistent morphology observed in TEM. The absence of large clusters provided additional evidence of good stabilization during synthesis [12, 13].

Preparation of AgNP-Loaded Hydrogel:

To make the hydrogel basis, Carbopol 940 was dissolved in distilled water at a concentration of 1-2 percent by weight while stirring constantly. To get a transparent gel, triethanolamine was used to neutralize the dispersion. The AgNP-loaded hydrogel was created by uniformly mixing the hydrogel with AgNPs, which were added at a concentration of 0.1% w/w. We checked the formulation's homogeneity, spreadability, viscosity, and pH [14].

Experimental Animals:

Healthy adult Swiss albino mice (20–25 g) of either sex were used for the study. The animals were kept in a typical laboratory setting with full access to food and water, with temperatures ranging from 25 ± 2°C to 65 ± 65% relative humidity and a 12 hour light/dark cycle. The protocols established by the institutional animal ethics committee (IAEC) were strictly adhered to during all experiments [15].

Induction of Burn Wound:

A ketamine solution (50 mg/kg, i.p.) was used to put the mice to sleep. A full-thickness burn wound was made by shaving the dorsal fur and then applying a pre-heated metal rod with a 1.5 cm

diameter to the skin for 10 seconds. To stop more tissue damage, sterile saline was quickly applied to the burn area [16].

Infection of Burn Wound:

A bacterial suspension containing about 10^8 CFU/mL of Staphylococcus aureus or Pseudomonas aeruginosa was added to the burn sites in a volume of 0.1 mL. A whole day had passed after infection had taken hold before therapy could begin [17].

Experimental Design:

The efficacy of the created formulation against microbes and its ability to cure wounds were assessed in four groups of six mice each, with the animals randomly assigned to each.

- **Group I (Control):** Received no treatment and served as the untreated control group.
- **Group II (Plain Hydrogel):** Treated with hydrogel base without active drug.
- **Group III (Standard):** Treated with commercially available silver sulfadiazine cream (1% w/w).
- **Group IV (Test):** Treated with silver nanoparticles (AgNPs)-loaded hydrogel.

Aseptically applied once daily for 14 days, the corresponding therapies were administered to burn wounds once infection had set in. In order to guarantee that the drug was exposed uniformly throughout the investigation, the treatment area was maintained constant. Wound healing progress, reduction in microbial load, and other evaluation parameters were tracked in all groups at predefined time intervals [18].

Evaluation Parameters:

1. Wound Contraction (%):

The decrease in wound area was assessed at designated intervals to evaluate the progression of wound healing. On days 0, 3, 7, 10, and 14, the wound area was quantified on graph paper subsequent to tracing it with a transparent overlay. To determine the wound surface area in square millimeters (mm^2), the wound margins were delineated on a sterile transparent sheet and subsequently transposed onto graph paper. This approach enabled precise and consistent measurement of wound size throughout time. The wound is healing appropriately if the area persists in diminishing. Increased percentage values are associated with accelerated wound contraction and enhanced therapeutic efficacy. To mitigate the likelihood of human error, we conducted each measurement thrice and calculated the average of the results [19]. We determined the rate of wound closure by estimating the percentage of contraction using the following formula:

$$\text{Wound Contraction (\%)} = \frac{\text{Initial Wound Area} - \text{Wound Area on Specific Day}}{\text{Initial Wound Area}} \times 100$$

2. Bacterial Load Estimation

The bacterial load in the wound tissues was evaluated at many time intervals to evaluate the antibacterial efficacy of the therapy. The animals in each cohort were euthanized on days 3, 7, and 14, and the tissues adjacent to the incisions were meticulously excised in an aseptic manner. In aseptic settings, the measured tissues were homogenized in sterile normal saline with a tissue homogenizer. Subsequently, the homogenates were serially diluted, and the resultant solutions were uniformly spread onto nutrient agar plates. Following 24 hours of incubation at 37°C, the plates were assessed for colony formation. The bacterial load was quantified as colony-forming units per gram (CFU/g) of tissue to measure the severity of the infection. The results indicated a significant reduction in CFU levels in the treated groups relative to the control group, demonstrating the formulation's effective antibacterial activity [20].

3. Epithelialization Period

The rate of wound healing was assessed by evaluating the epithelialization duration. The duration required for the complete coverage of the wound surface by new epithelium, the natural detachment of the scab without exposing any raw tissue, and the overall healing of the wound was delineated. The animals were observed daily, and the date of complete recovery was recorded. A reduced epithelialization period indicated enhanced wound healing and therapeutic efficiency [21].

4. Histopathological Analysis

Granulation tissue samples were collected from the wound site after 14 days to microscopically assess the healing process. To ensure preservation, the materials were immediately fixed in 10% neutral buffered formalin. The tissues were processed post-fixation through processing, embedding in paraffin, and sectioning into thin slices approximately 4-5 µm thick. Subsequently, the sections underwent the H&E staining technique. Improved healing outcomes were demonstrated by superior histological architecture, as evidenced by comparative research among several groups, which illuminated the degree of tissue repair and regeneration [22].

Statistical Analysis:

All experimental data were expressed as the mean plus or minus the standard deviation (SD). One-way analysis of variance (ANOVA) was employed to identify group differences, and Tukey's post hoc test was utilized for multiple comparisons. Substantial disparities between treatment groups were evidenced by a p-value below 0.05.

Results:

1. UV–Visible Spectroscopy:

Ultraviolet-visible spectroscopy, grounded in the principle of surface plasmon resonance (SPR), facilitated the verification of silver nanoparticles' synthesis. The absorbance spectra of the synthesized AgNPs were recorded in the 300-700 nm region. A characteristic feature of spherical silver nanoparticles is the existence of an absorption peak at λmax = 420 nm. The collective oscillation of conduction electrons on the nanoparticle surface in response to incident light results in the emergence of this peak. The effective synthesis of AgNPs was further evidenced by the reaction mixture changing color from pale yellow to brown. Minimal aggregation and a pronounced peak indicate that the particles were of consistent size. The synthesized nanoparticles were confirmed to be pure and stable, since the spectra exhibited no additional peaks (Figure 1).

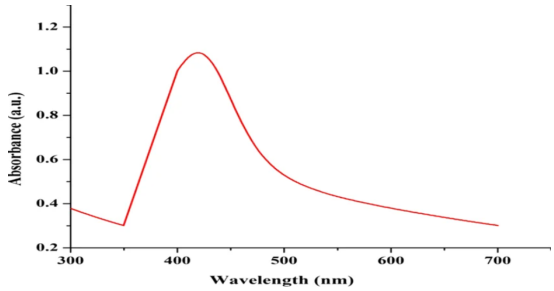

Figure 1. UV–Visible absorption spectrum of the prepared AgNPs

2. Characterization of Silver Nanoparticles (AgNPs)

Further investigation by dynamic light scattering (DLS) revealed that the nanoparticles exhibited a narrow and uniform size distribution, with an average particle size of 48.7 ± 5.8 nm and a polydispersity index (PDI) of 0.24. The low PDI score signifies that the particles are uniformly distributed and exhibit minimal aggregation. The AgNPs exhibited a sufficiently robust negative surface charge, as evidenced by a zeta potential measurement of −29.6 ± 2.1 mV. The result indicates that the colloidal solution is stable due to electrostatic repulsion, which prevents particle aggregation and ensures long-term dispersion stability. Morphological investigation by transmission electron microscopy (TEM) confirmed that the nanoparticles were predominantly spherical, with sizes ranging from fifteen to fifty nanometers (nm). The transmission electron microscopy (TEM) images gave additional confirmation of the endurance and homogeneity of the generated nanoparticles, showing uniformly distributed particles devoid of noticeable aggregation (Figure 2).

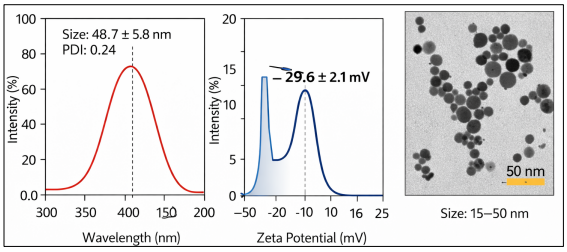

Figure 2: DLS size distribution, zeta potential, and TEM images of the synthesized AgNPs

3. Wound Contraction (%)

Throughout the 14-day study, wound contraction was shown to rise in all groups, indicating a gradual healing process of burn wounds. Conversely, at all time intervals, the control, plain hydrogel, and standard treatment cohorts exhibited significantly reduced wound contraction compared to the AgNP-loaded hydrogel cohort. In comparison to the control group (11.8 ± 1.3%) and other groups, the AgNP-treated group exhibited a significantly higher contraction of 27.9 ± 2.0% during the initial phase (day 3). During the experiment, this trend continued, with notable enhancements observed on days 7 (66.1 ± 3.0%) and 10 (83.5 ± 3.4%), indicating an acceleration of the healing process. On day 14, the group administered AgNP hydrogel exhibited a wound contraction of 92.8 ± 2.7%, significantly surpassing the control group (55.1 ± 3.0%), plain hydrogel (72.6 ± 3.3%), and conventional treatment (85.7 ± 3.6%) ($p < 0.001$). The enhanced wound contraction in the AgNP-treated group likely resulted in improved tissue regeneration and expedited wound closure (Table 1 & Figure 3).

Table 1: Wound Contraction (%)

Day	Control	Plain Hydrogel	Standard	AgNP Hydrogel
0	0.0 ± 0.0	0.0 ± 0.0	0.0 ± 0.0	0.0 ± 0.0
3	11.8 ± 1.3	18.1 ± 1.5	22.6 ± 1.7	27.9 ± 2.0*
7	29.4 ± 2.1	41.5 ± 2.4	53.2 ± 2.7	66.1 ± 3.0**
10	43.6 ± 2.6	59.2 ± 2.9	71.8 ± 3.2	83.5 ± 3.4**
14	55.1 ± 3.0	72.6 ± 3.3	85.7 ± 3.6	92.8 ± 2.7***

(*$p < 0.05$, **$p < 0.01$, ***$p < 0.001$ vs control)

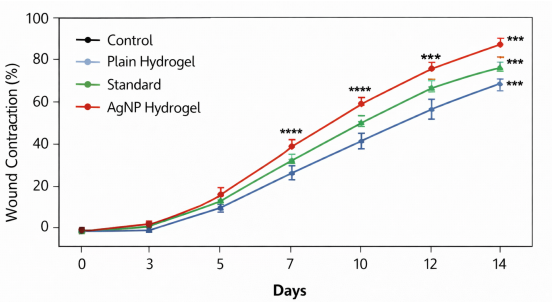

Figure 3: Wound contraction profile of different treatment groups over the study duration

4. Bacterial Load Estimation

We assessed the bacterial load in wound tissues at various time intervals to evaluate the antibacterial efficacy of the treatments. The bacterial load diminished with time in all treatment groups relative to the control group. On day 3, the bacterial count in the AgNP-loaded hydrogel treatment group was 4.0 ± 0.3 × 10^6 CFU/g, significantly lower than the control group (8.3 ± 0.6 × 10^6 CFU/g) and all other treatment groups. This indicates that the antimicrobial effect commences promptly. Relative to the standard (3.3 ± 0.3 × 10^6 CFU/g) and plain hydrogel groups, the bacterial load in the AgNP-treated group markedly decreased to 1.7 ± 0.2 × 10^6 CFU/g on day 7. The AgNP hydrogel group exhibited the greatest significant reduction in microbial load on day 14, recording the lowest bacterial count (0.4 ± 0.1 × 10^6 CFU/g). Relative to the untreated control group, exhibiting bacterial loads of 6.0 ± 0.4 × 10^6 CFU/g ($p < 0.001$), this indicates a reduction of approximately three logarithmic units. The enhanced efficacy against bacteria at the burn site stemmed from the broad-spectrum bactericidal properties of the silver nanoparticles included into the hydrogel (Table 2 & Figure 4).

Table 2: Bacterial Load (CFU × 10^6/g Tissue)

Day	Control	Plain Hydrogel	Standard	AgNP Hydrogel
3	8.3 ± 0.6	7.1 ± 0.5	5.9 ± 0.4	4.0 ± 0.3*
7	7.1 ± 0.5	5.4 ± 0.4	3.3 ± 0.3	1.7 ± 0.2**
14	6.0 ±	3.8 ±	1.6 ±	0.4 ±

	0.4	0.3	0.2	0.1***

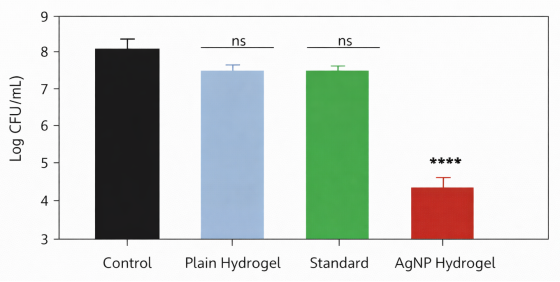

Figure 4: Reduction in bacterial load across different treatment groups

5. Epithelialization Period

The epithelialization period is a crucial indicator of wound healing speed, defined as the duration required for newly formed epithelium to completely cover the wound surface and for the scab to detach naturally. The duration of epithelialization was markedly reduced in all treatment groups compared to the control group in this study. The cohort of hydrogels infused with AgNPs had the most rapid epithelialization period, indicating accelerated wound closure and enhanced tissue regeneration. The control group exhibited delayed healing, with an epithelialization length of 16.3 ± 1.2 days. The duration was significantly decreased to 14.0 ± 1.0 days following treatment with basic hydrogel, suggesting that the moist wound environment exerted a beneficial influence. The epithelialization period was 12.5 ± 0.9 days, indicating a further improvement in the healing process within the standard therapy group (silver sulfadiazine). Notably, in comparison to the control group, the AgNP hydrogel group exhibited the most rapid epithelialization, achieving complete wound closure in 11.1 ± 0.7 days ($p < 0.001$). The accelerated healing process may be attributed to the antibacterial characteristics and enhanced cellular regeneration induced by silver nanoparticles (Table 3 & Figure 5).

Table 3: Epithelialization Period (Days)

Group	Epithelialization Period (Days)
Control	16.3 ± 1.2
Plain Hydrogel	14.0 ± 1.0
Standard	12.5 ± 0.9
AgNP Hydrogel	11.1 ± 0.7***

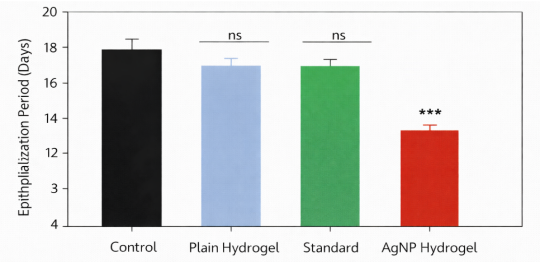

Figure 5: Comparative epithelialization periods among different treatment

6. Histopathological Analysis

On the fourteenth day, the wound tissues underwent histological examination to assess the extent of tissue regeneration and healing. The AgNP-loaded hydrogel group exhibited superior histological architecture compared to the other treatment groups, as indicated by the results. The control group's tissue slices exhibited insufficient collagen deposition, pronounced inflammatory cell infiltration, and disrupted dermal and epidermal architecture, indicative of inadequate and delayed healing. Partial epithelialization, decreased inflammatory infiltration, and initial collagen synthesis were noted in the plain hydrogel group, suggesting that healing was occurring due to the hydrogel's moist environment. This group exhibited slight enhancement. Notable advancements, including enhanced epithelial layer formation, increased collagen deposition, and less inflammation, were observed in the standard therapy group (silver sulfadiazine), indicating effective wound healing. The group administered AgNP-loaded hydrogel had the greatest advanced healing (Figure 6). This group exhibited substantial fibroblast proliferation, considerable neovascularization, minimal inflammatory cell infiltration, and dense, well-structured collagen fibers. The epidermis exhibited a smooth, continuous look, indicating near-complete tissue regeneration. The findings indicate that the AgNP-loaded hydrogel significantly enhances wound healing by diminishing inflammation, fostering cellular proliferation, and facilitating angiogenesis.

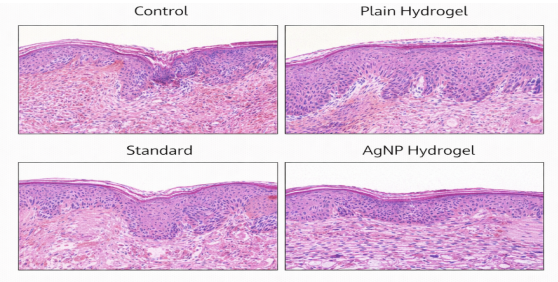

Figure 6: Histopathological (H&E-stained) sections of wound tissues from different treatment groups

Discussion:

The heightened susceptibility to microbial colonization and delayed healing render burn wound infections a considerable therapeutic challenge. The findings indicate that the hydrogel infused with silver nanoparticles (AgNPs) exhibited superior therapeutic efficacy compared to the control and traditional therapies regarding in vivo antibacterial effectiveness and wound healing potential [20].

The outcomes of DLS, zeta potential, TEM, and UV-Visible spectroscopy, which indicated a peak at around 420 nm, confirmed the formation of stable, uniformly dispersed silver nanoparticles. The particle size range (15-50 nm by TEM; about 48 nm via DLS) and negative zeta potential (~−29 mV) indicate favorable colloidal stability and suitability for biological applications. To enhance antibacterial efficacy, certain physicochemical characteristics are essential. Smaller and more uniformly dispersed nanoparticles possess a greater surface area and exhibit enhanced interactions with microbial cells [21].

The study on wound contraction revealed that the cohort treated with AgNP hydrogel exhibited a significantly accelerated rate of wound closure. By day 14, wound contraction exceeded 92% to 93%, significantly outpacing both the control group and traditional treatment. The combined effects of antimicrobial activity and the stimulation of biological processes, such as fibroblast proliferation and collagen synthesis, may elucidate this enhanced contraction. The hydrogel's moist environment facilitates tissue healing and re-epithelialization [22].

The assessment of bacterial load indicated that the AgNP-treated group exhibited a significantly reduced microbial burden compared to the control group, with an approximate 3-log decrease in CFU. This discovery highlights the potent antibacterial properties of silver nanoparticles against several microbes. The mechanism of action is believed to entail the generation of reactive oxygen species (ROS), interference with DNA replication and protein synthesis, and rupture of the bacterial cell membrane. The AgNP hydrogel exhibited superior and prolonged antibacterial efficacy compared to silver sulfadiazine, likely attributable to enhanced bioavailability and focused action [23-24].

The AgNP-treated group exhibited accelerated wound healing and regeneration of the epidermal layer, with a significant reduction in the epithelialization period to around 11 days. This expedited healing is linked to decreased infection, accelerated keratinocyte migration, and augmented extracellular matrix formation [26-28].

The findings were additionally validated by histological analysis, which demonstrated that the AgNP hydrogel group displayed well-structured collagen fibers, increased fibroblast activity, enhanced neovascularization, and little inflammatory infiltration. Conversely, the control group had indications of persistent inflammation and disordered tissues. Histological enhancements in the treatment group suggest that AgNPs not only suppress infection but also promote angiogenesis and tissue remodeling, both critical processes for effective wound healing [29-33].

Conclusion:

Hydrogel dressings coated with silver nanoparticles (AgNPs) significantly reduced microbial numbers and improved wound healing rates in a live burn wound infection model, according to recent research. Accurate production and characterization of AgNPs have validated their favorable physicochemical properties, which include nanoscale size, homogeneous dispersion, and excellent colloidal stability. The hydrogel that was infused with AgNPs showed improved wound contraction (~92-93%), a notable drop in bacterial load (~3-log CFU decrease), and a significantly quicker time of epithelialization (~11 days)

compared to the control and standard treatments. The histology results showed that the tissue regeneration was superior, with less inflammation, better angiogenesis, more structured collagen deposition, and more multiplication of fibroblasts. The results show that the hydrogel loaded with AgNPs has two benefits as a therapeutic agent: it speeds up wound healing and it handles infections well. This formulation shows great promise as an improved option for treating burn wounds that have become infected. Greater investigation into its therapeutic potential and safety over the long term is required before it can be considered effective in humans.

Funding:
None

Conflict of Interest:
None

REFERENCES:

1. Atiyeh BS, Costagliola M, Hayek SN, Dibo SA. Effect of silver on burn wound infection control and healing. Burns. 2007;33(2):139–48.
2. Rai M, Yadav A, Gade A. Silver nanoparticles as a new generation of antimicrobials. Biotechnol Adv. 2009;27(1):76–83.
3. Franci G, Falanga A, Galdiero S, Palomba L, Rai M, Morelli G, et al. Silver nanoparticles as potential antibacterial agents. Molecules. 2015;20(5):8856–74.
4. Boateng JS, Matthews KH, Stevens HN, Eccleston GM. Wound healing dressings and drug delivery systems: a review. J Pharm Sci. 2008;97(8):2892–923.
5. Gupta A, Silver S. Silver as a biocide: will resistance become a problem? Nat Biotechnol. 1998;16(10):888–90.
6. Morones JR, Elechiguerra JL, Camacho A, Holt K, Kouri JB, Ramírez JT, et al. The bactericidal effect of silver nanoparticles. Nanotechnology. 2005;16(10):2346–53.
7. Pal S, Tak YK, Song JM. Does the antibacterial activity of silver nanoparticles depend on the shape of the nanoparticle? Appl Environ Microbiol. 2007;73(6):1712–20.
8. Lansdown AB. A review of the use of silver in wound care: facts and fallacies. Br J Nurs. 2004;13(6):S6–19.
9. Kim JS, Kuk E, Yu KN, Kim JH, Park SJ, Lee HJ, et al. Antimicrobial effects of silver nanoparticles. Nanomedicine. 2007;3(1):95–101.
10. Klasen HJ. Historical review of the use of silver in the treatment of burns. Burns. 2000;26(2):117–30.
11. Thomas S, McCubbin P. An in vitro analysis of the antimicrobial properties of 10 silver-containing dressings. J Wound Care. 2003;12(8):305–8.
12. Zhang L, Pornpattananangkul D, Hu CM, Huang CM. Development of nanoparticles for antimicrobial drug delivery. Curr Med Chem. 2010;17(6):585–94.
13. Percival SL, Bowler PG, Russell D. Bacterial resistance to silver in wound care. J Hosp Infect. 2005;60(1):1–7.
14. Li WR, Xie XB, Shi QS, Duan SS, Ouyang YS, Chen YB. Antibacterial effect of silver nanoparticles on Staphylococcus aureus and Escherichia coli. Appl Microbiol Biotechnol. 2010;85(4):1115–22.
15. Singh R, Singh D. Chitin membranes containing silver nanoparticles for wound dressing application. Int Wound J. 2014;11(3):264–8.
16. Ahmed S, Ahmad M, Swami BL, Ikram S. A review on plants extract mediated synthesis of silver nanoparticles. J Adv Res. 2016;7(1):17–28.
17. Boateng JS, Catanzano O. Advanced therapeutic dressings for effective wound healing—a review. J Pharm Sci. 2015;104(11):3653–80.
18. Leaper DJ. Silver dressings: their role in wound management. Int Wound J. 2006;3(4):282–94.
19. Wilkinson LJ, White RJ, Chipman JK. Silver and nanoparticles of silver in wound dressings: a review of efficacy and safety. J Wound Care. 2011;20(11):543–9.

20. Kalishwaralal K, BarathManiKanth S, Pandian SR, Deepak V, Gurunathan S. Silver nanoparticles impede the biofilm formation by Pseudomonas aeruginosa. Colloids Surf B Biointerfaces. 2010;79(2):340–4.
21. Galdiero S, Falanga A, Vitiello M, Cantisani M, Marra V, Galdiero M. Silver nanoparticles as potential antiviral agents. Molecules. 2011;16(10):8894–918.
22. Veerasamy R, Xin TZ, Gunasagaran S, Xiang TF, Yang EF, Jeyakumar N, et al. Biosynthesis of silver nanoparticles using mangosteen leaf extract and evaluation of antimicrobial activities. J Saudi Chem Soc. 2011;15(2):113–20.
23. Shanmugam N, Rajan KS, Kumar TS. Synthesis of silver nanoparticles and their biomedical applications. Int J Pharm Sci Rev Res. 2014;25(1):52–7.
24. Varaprasad K, Mohan YM, Vimala K, Raju KM. Synthesis and characterization of hydrogel-silver nanoparticle-curcumin composites for wound dressing and antibacterial application. J Appl Polym Sci. 2011;121(2):784–96.
25. Dhivya S, Padma VV, Santhini E. Wound dressings—a review. Biomedicine. 2015;5(4):22.
26. Sood A, Granick MS, Tomaselli NL. Wound dressings and comparative effectiveness data. Adv Wound Care. 2014;3(8):511–29.
27. Behera J, Keservani R K, Yadav A, Tripathi M and Chadoker A, Methoxsalen loaded chitosan coated microemulsion for effective treatment of psoriasis. Int. J. Drug Del. 2010, 2, 159-167.doi:10.5138/ijdd.2010.0975.0215.02025
28. Khulbe P, Singh D M, Aman A, Ahire E D and Keservani R K, The emergence of nanocarriers in the management of diseases and disorders. Community Acquired Infection 2023, 10. https://doi.org/10.54844/cai.2022.0139
29. Keservani Raj K and Gautam Surya Prakash, Formulation and evaluation of baclofen liposome vesicles using lecithin. ARS Pharmaceutica 2020, 61 (3), 175-180. http://dx.doi.org/10.30827/ ars.v61i3.15279
30. Keservani Raj K and Gautam Surya Prakash, Skeletal muscle relaxant activity of different formulation of span 60 niosome. ARS Pharmaceutica 2022, 63 (1), 32-44. https://dx.doi.org/10.30827/ars.v63i1.22264
31. Keservani R K, Sharma A K and Ramteke S, Novel vesicular approach for topical delivery of baclofen via niosomes. Lat. Am J. Pharm. 2010, 29, 1364-1370.
32. Keservani R K and Sharma A K, Nanoemulsions: Formulation insights, applications and recent advances. Nanodispersions for Drug Delivery 2018, 71-96. eBook ISBN-9781351047562
33. Bharti A D, Keservani R K, Sharma A K, Kesharwani Rajesh K and Mohammed G H, Formulation and in vitro characterization of metoprolol tartrate loaded chitosan microspheres. Ars Pharmaceutica 2012, 53-3, 13-18.